Relationship between active fault landform and surface rupture accompanied with 2016 Kumamoto Earthquake

*Yasuhiro Kumahara[1]

1. Graduate School of Education, Hiroshima University

On 16 April 2016, a Mw=7.0 (Mjma=7.3) earthquake hit from Kumamoto city to the Aso volcanic Caldera in central Kumamoto Prefecture, central Kyushu. Prior to the 16 April earthquake, the 14 April Mw=6.2 (Mjma=6.5) earthquake was also generated at close to the epicenter of the 16 April Earthquake in east of Kumamoto City. It is well known that there is a north part of the Futagawa-Hinagu fault system (FHFS), mapped by previous studies (e.g. Research group for active tectonics in Kyushu ed, 1989; Nakata and Imaizumi ed, 2002) in the epicentral area. The photo-interpretation method is common to map the fault trace in Japan. Because the traces of the FHFS run below the dense forest and village, the cumulative offset along the FHFS was not mapped sufficiently. The 2 m-grid Digital Elevation Model along the FHFS acquired by the GSI provided us the firm evidences of cumulative right-lateral strike-slip along the FHFS, and also Idenokuchi fault, parallel to the Futagawa fault. Here we show the relationship between tectonic landform and surface rupture accompanied with Kumamoto Earthquake.

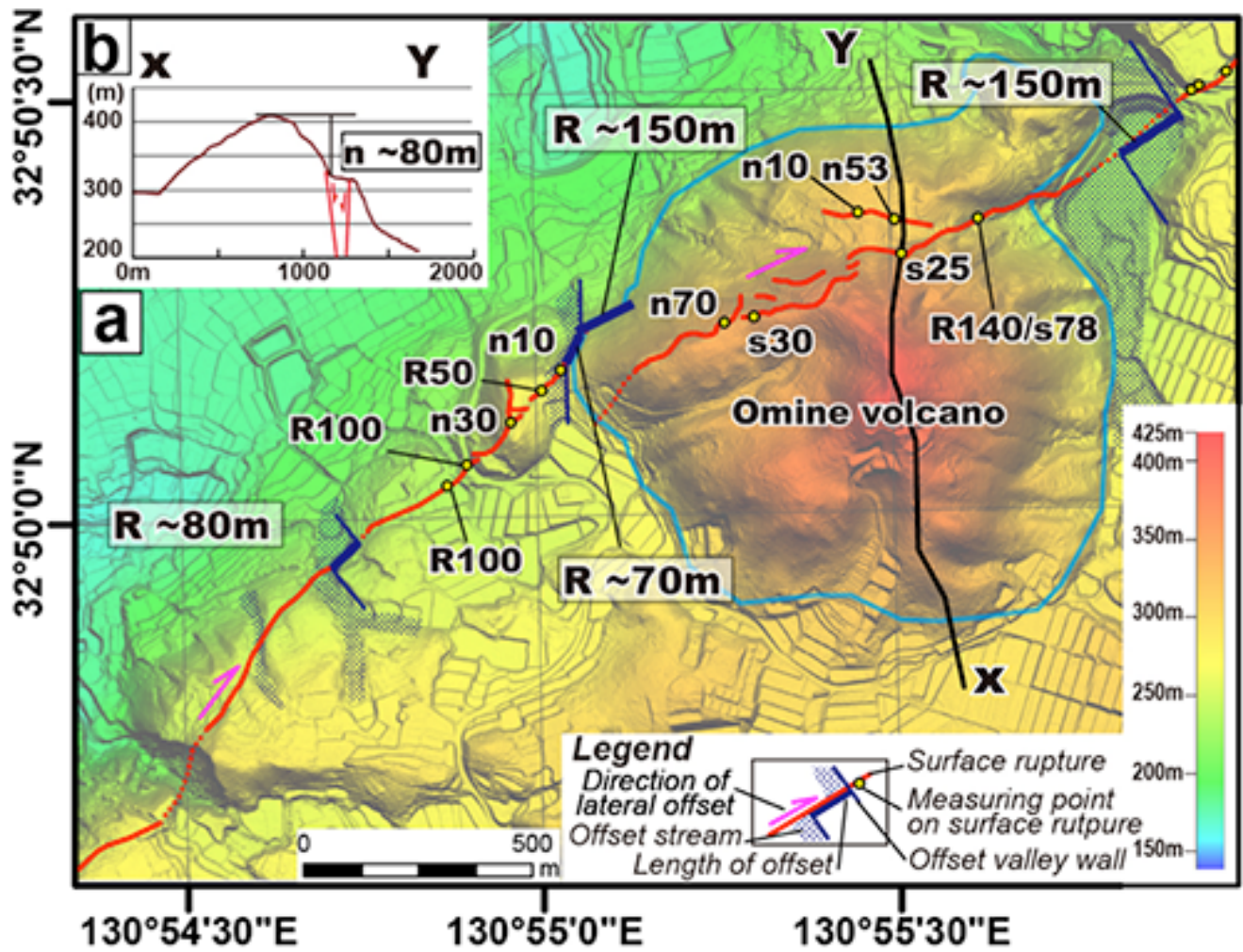Keywords: Kumamoto Earthquake, Surface rupture, Active fault

Figure 1 surface rupture with displacement and cumulative offset on the rupture in Oomine, Nishihara.

Utilizing 8K Super Hi-Vision for Disaster Mitigation and Geosciences: reporting from the 2016 Kumamoto earthquake in Japan

*MASARU YAMAGUCHI[1]

1. NHK Japan Broadcasting Corporation,Broadcasting Culture Research Institute

NHK (Japan Broadcasting Corporation) launched test broadcasting of 4K/8K(super hi-vision) in 2016. This presentation clarifies the fact that 8K, ultra-high definition image,16 times that of HDTV(2K),is useful for not only broadcasting but also disaster research and geosciences in terms of remote sensing, space information.
NHK used an 8K small camera in aerial filming of areas along active faults that were severely damaged immediately after the 2016 Kumamoto earthquake. As we had active fault scientists analyze the footage, undiscovered earthquake faults and raptures were found, which were reported in an NHK's TV program. This served as the first utilization of disaster analyses of 8K images in disaster reporting in media.
Aerial filming using an 8K camera enables discovery of ruptures as small as a few centimeters from an altitude of 400 meters, and provides "higher resolution" than aerial photography and "wider angles of view" than 4K drones. Since ruptures may cause a variety of disasters, there are high expectations for the utilization of 8K images in DRR. 8K images also allow the observation of each individual's "move," which will be effective for life-saving and search operations and detecting temporary shelters. 8K's "oblique bird's-eye views" provides vertical information that will make it easier to survey collapsed buildings, and its graphics data can be utilized for making "3D models" and "crisis maps."
Reference: Yamaguchi(2017) Possibility of Utilizing 8K Super Hi-Vision for Disaster Risk Reduction The NHK Monthly Report on Broadcast Research (Japanese)
http://www.nhk.or.jp/bunken/english/reports/summary/201701/01.html

Keywords: active fault, 8K Super Hi-Vision, remote sensing, Media, Japan broadcasting corporation, disaster

The 8K Super Hi-Vision system supports higher frame rates to enable vivid reproduction of the subject, in addition to ultra-high definition video of approximately 33 megapixels. Also, the wider color gamut and greater bit depth have made it an ultimate TV broadcasting system capable of reproducing bright colors more accurately.

8K Super Hi-Vision image

Aspect ratio	16 : 9
Pixel number	7,680 × 4,320
Frame rate	120, 119.88, 60, 59.94 Hz Progressive
Scanning	Progressive
Bit depth	10, 12 bit
Color gamut	Wide gamut system colorimetry
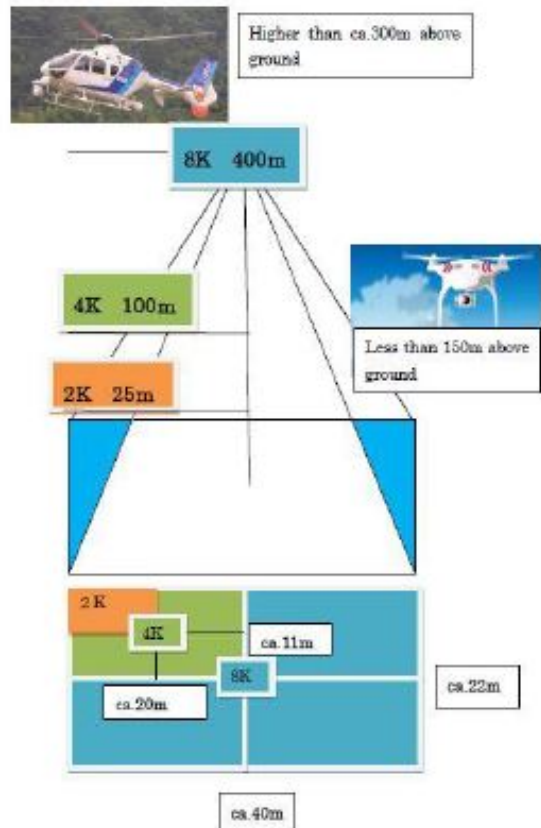
resolution: The ground pixel size

5 mm : 8K (this study)

100 mm : aerial photograph of Geospatial Information Authority of Japan

You can watch flying butterfly on the ground shot by 8K camera from 400m high above ground.

Estimation of Slip Velocity Function for the Region Shallower than Seismogenic Layer

*Tanaka Shinya[1], Kazuhito Hikima[2], Yoshiaki Hisada[3]

1. Tokyo Electric Power Services Co., Ltd., 2. Tokyo Electric Power Company, 3. Kogakuin University

1. Introduction

The 2016 Kumamoto earthquake (Mw7.0) generated the expensive surface faulting, and recorded characteristic near-fault strong motions. For this reason the main attention has been directed to estimation of near-fault strong ground motion and the fling step. The theoretical method is widely used for estimation of near-fault strong ground motion, but little is known about slip velocity function required for estimation, especially the region shallower than seismogenic layer. According to Hikima et al. (2015), slip velocity function in the shallow section of the faulting area are different from that in the deep section. The purpose of this study is to estimate slip velocity function for the region shallower than seismogenic layer using near-fault strong ground motions and source fault models.

2. Study on the 1999 Chi-Chi Earthquake

The 1999 Chi-Chi earthquake (Mw7.6) recorded near-fault strong ground motions. TCU068, TCU102 are lying on the hanging wall, and TCU052 is lying on the foot wall. We simulated these observation records by theoretical method. Figure 1 shows slip velocity function identified by Wu et al. (2001) close to strong-motion stations. Figure 2 shows comparison of synthetic and observation waveforms fittings. Figure 2 include three sets of synthetic waves; the top waves (case1) simulated using source fault model by Wu et al.(2001). The middle waves (case2) correspond to simulated using only subfaults close to strong-motion stations, about 10km long and 6km wide. The bottom waves (case3) correspond to simulated using subfaults close to strong-motion stations similarly case2. In addition, we used average slip of subfaults close to strong-motion stations and a simple triangle time window as slip velocity function. For TCU068 and TCU102 lying on the hanging wall, the synthetic waves of case1 and case2 are in good agreement with observation records. Subfaults close to strong-motion stations dominates in velocity and displacement waveforms. In addition, observation velocity waveforms are very similar to slip velocity function of subfaults close to strong-motion stations. Since we approximate slip velocity function as a simple triangle time window (that is case3). We estimated that the values for duration of triangle time window as slip velocity function and average slip of subfaults close to TCU068 were 5sec and 8.2m, TCU052 were 7sec and 12.1m, respectively. As a result, the synthetic waves of case3 are in good agreement with observation records.

Whereas, observation velocity waveforms of TCU052 lying on the foot wall has a different from slip velocity function. In addition, it cannot be said that subfaults close to strong-motion stations dominates in velocity waveforms. One reason for this is the greater are that displacement on the footwall is smaller than on the hanging wall because of low dip angle (about 30˚). It was noted that it is difficult to approximate slip velocity function from only near-fault strong ground motions. Besides, it may be suspected that accuracy of slip velocity function is low if strong-motion stations lie only on the foot wall of low-angle fault. Incidentally, we estimated that the values for duration of triangle time window as slip velocity function and average slip of subfaults close to TCU102 were 6sec and 9.6m, respectively.

3. Estimation of Slip Velocity Function

In light of these considerations we estimated slip velocity function for the region shallower than seismogenic layer for other earthquakes in the same way as 1999 Chi-Chi earthquake. It was found that

the duration of triangle time window as slip velocity function correlates positively with average slip of subfaults close to strong-motion stations as shown in Fig.3. Further studies for more earthquakes are needed in order to improve the accuracy of estimation of near-fault strong ground motion.

Keywords: Near source region, Slip velocity function, the Seismic Waveform Inversion, Strong ground motion prediction
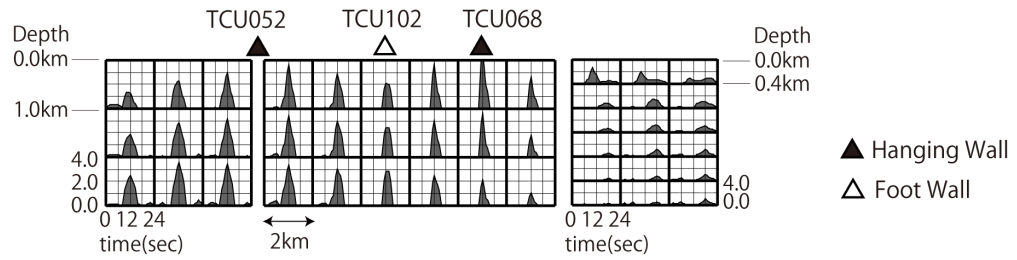
Figure 1. Slip velocity function by Wu et al.(2001) near strong-motion stations
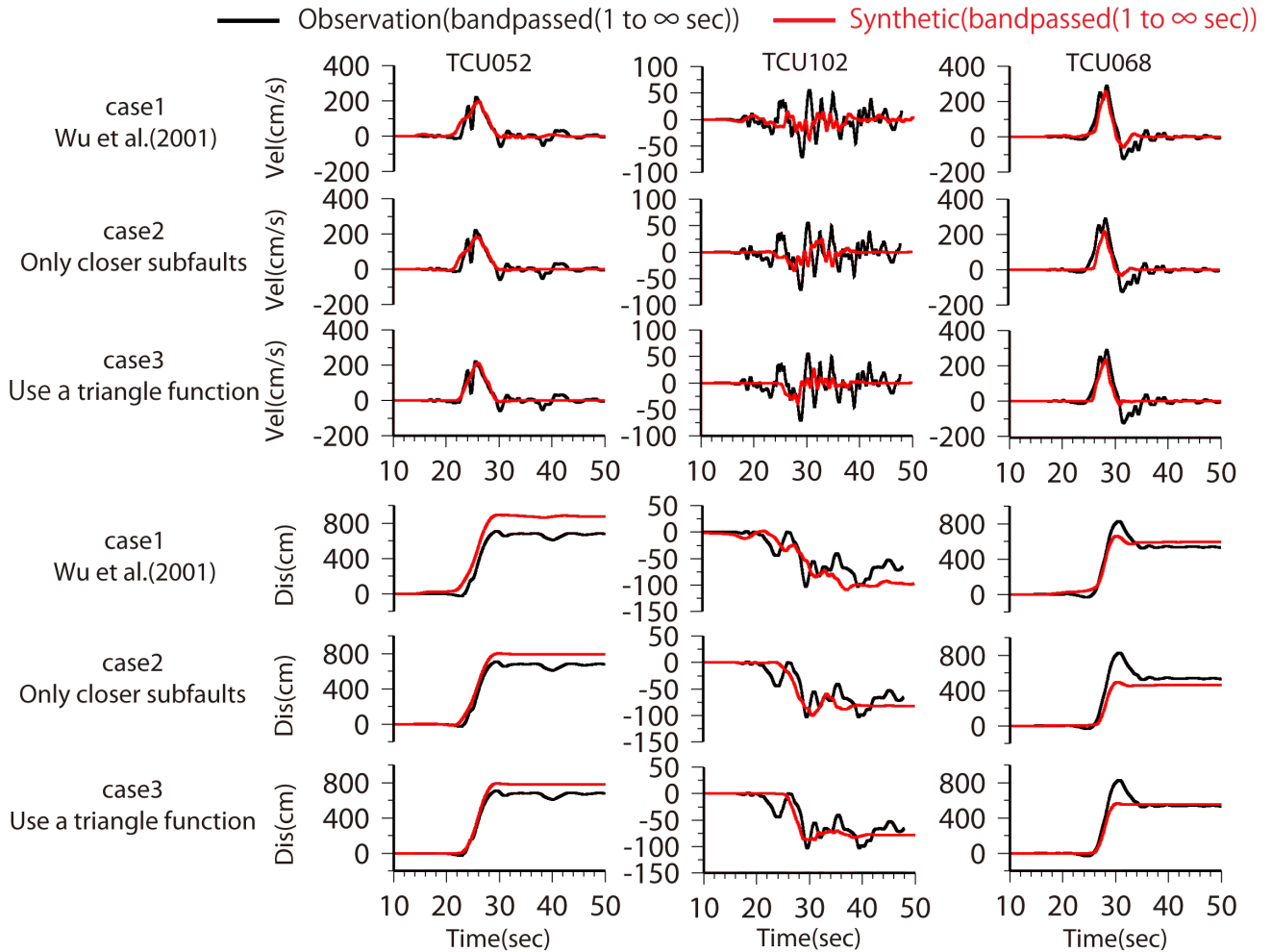in the northern part of 1999Chi-Chi

Figure 2. Comparison of synthetic and observation waveform fittings (NS component, 1999Chi-Chi)
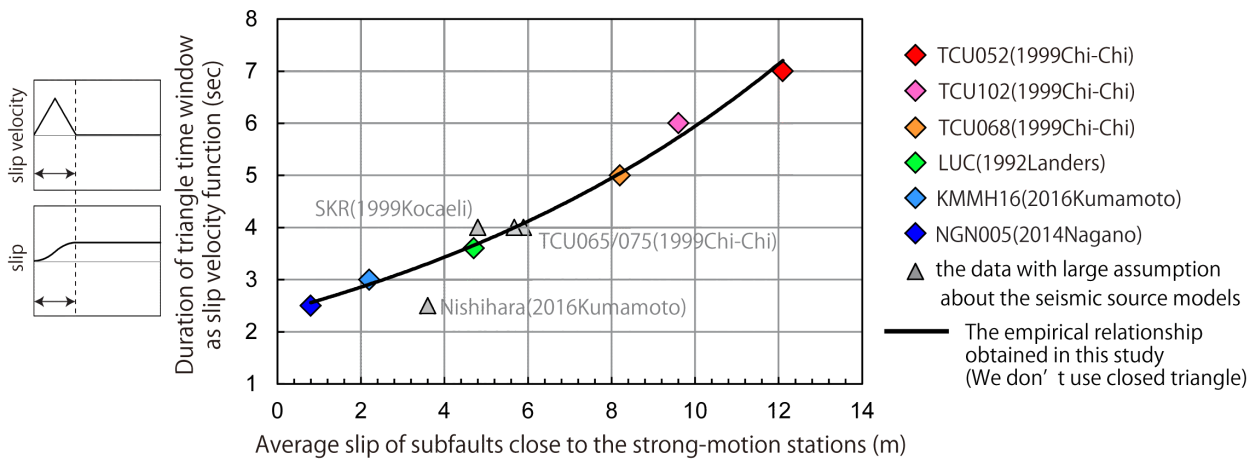

Figure 3. Relationships among slip velocity function and slip in shallower region than the seismogenic layer

A study on modeling method of active faults with surface rupture for strong ground motion evaluation

*Nobuyuki Morikawa[1], Hiroyuki Fujiwara[1], Asako Iwaki[1], Takahiro Maeda[1]

1. National Research Institute for Earth Science and Disaster Resilience

In the strong-motion evaluation, the emphasis was mainly on modeling of short period strong-motion generation, the source faults was within the seismogenic layer, and its upper end was not 0km (surface). However, it is necessary to model the upper end of the source fault at 0km up even in strong-motion evaluation for earthquakes occurring in active faults where clear surface fault is identified.

As a first step to extend the source fault model to the ground surface in strong-motion evaluation, here we considered three models for the main shock of the 2016 Kumamoto earthquake (Mw=7.0) as below;
Model-1: The upper end and width of the source fault are 0km and 18km,
Model-2: The upper end and width of the source fault are 2km and 18km,
Model-3: The upper end and width of the source fault are 2km and 16km.
We assumed that the length of the source fault was 34km, which was same as the length of recognized surface fault, and seismic moment was 4.5e19 Nm in all models. And we applied the strike and dip as same as the model for the Futagawa segment of Futagawa fault zone by Headquarters for Earthquake Research Promotion (2014). Source parameters. For model-1, we set up two types of models. The one was using slip velocity time functions by Nakamura and Miyatake (2000) for whole source fault (Model-1NM). The other was using smoothed ramp type slip time functions for shallower than the top of the seismogenic zone (2km; Model-1SR). The locations of hypocenter and asperities were common to all models.

We performed strong-motion simulations for the above four source models using a 3-D underground velocity structure model J-SHIS V2 (Fujiwara et al., 2012). The main results are follows.
1. The difference of strong-motion distribution between Model-1 and others can be seen at region where distance from surface fault is within 2km.
2. There is almost no difference in strong-motion distribution at region where distance from surface fault is farther than 2km.
3. In Model-1NM, a abnormal waveform appears at some sites. It causes extremely large PGV and/or JMA seismic intensity.
We conclude that strong-motion evaluation for earthquakes in active faults whose the upper end of the source fault is 0km by using a smoothed ramp type slip time function for shallower than the seismogenic zone can provide appropriate results comparable to previous evaluations. However, it is necessary to establish a detailed modeling method of the position and shape of the source fault, the slip velocity time function at shallower part of the source fault.

Keywords: The 2016 Kumamoto earthquake, surface fault, strong-motion evaluation

Ground motion amplification obtained with microtremor, aftershock and borehole measurements in heavily damaged zone in the Mashiki town, Kumamoto prefecture

*Masayuki Yoshimi[1], Hiroyuki Goto[2], Yoshiya Hata[3], Yoshikazu Shingaki[4], Takashi Hosoya[5], Sachiko Morita[5], Takeshi Sugiyama[6], Tetsuyoshi Tokumaru[6]

1. Geological Survey of Japan, AIST, 2. DPRI, Kyoto University, 3. Osaka University, 4. TEPSCO, 5. Chuo-Kaihatu Corporation, 6. Tokumaru PE office

Heavily damaged zone by the ground motion of the 2016 Kumamoto earthquake, Japan, was recognized in the downtown area of the Mashiki town, Kumamoto prefecture. Five records of the mainshock in/around the zone show that the ground motion in the zone were about 2-3 times stronger than that observed at KMMH16 in terms of the linear response around the period 1 sec. (Hata et al., 2016), which might explain difference of the damage. Goto et al. (2016, 2017) demonstrated that the nonlinear response of the shallower soil (down to 50 m as much) owed much to the amplification.
We conducted borehole survey (Yoshimi et al., 2016, 2017; Shingaki et al., 2017), aftershock and microtremor observation at three sites in the damaged zone. Site amplification characteristics of those sites in linear and nonlinear regime will be demonstrated.

Keywords: 2016 Kumamoto Earthquake, Ground amplification, Aftershock observation, Borehole survey, nonlinear site response

Relationship between subsurface structure and large-scale fissures in the northwestern region in Aso valley caused by the 2016 Kumamoto earthquake

*Issei Doi[1], Toshitaka Kamai[1], Satoshi Goto[2], Ryokei Azuma[3], Takahiro Ohkura[4], Hidehiko Murao[5], Kenji Mima[6]

1. Disaster Prevention Research Institute, 2. Integrated Graduate School of Medicine, Engineering, and Agricultural Sciences, Yamanashi University, 3. Faculty of Engineering, Osaka Institute of Technology, 4. Graduate School of Science, Kyoto University, 5. Murao Chiken, 6. Ohta Geo Research. Co., Ltd.

In accompanied with the 2016 Kumamoto earthquake, fissures with the length and the height a few hundred meters and two meters, respectively, emerged in Aso valley (inside the Aso caldera). In this area, the top layer consists of sediments in the caldera lake created by Aso-4 eruption with the thickness a few tens of meters. InSAR and seismic data show that the region with the size of 1-4 square meter moved 1-2 m northward horizontally during strong motion of the mainshock (Fujiwara et al., 2016; Doi et al., 2016). We investigated the mechanism of the movement of these regions by estimating subsurface structure beneath this area.

Two station spatial auto-correlation (2ST-SPAC) method (Hayashi and Craig, 2016) was applied to estimate subsurface structure using ambient noises. We succeeded to estimate the S-wave velocity structure to the depth of 130 m in and around the regions with fissures. In the regions where large scale fissures were developed, a layer with S-wave velocity less than 150 m/s lay from the surface to the depth of 60 m, followed by two layers with 250 m/s and 300 m/s at depths of 60-90 m and 90-130 m, respectively. This low-velocity layer was considered to represent soft sediments in the caldera lake due to Aso-4 eruption and consistent with the nearby boring profile. Two relatively higher layers might correspond to lava layers after Aso-4 eruption. Moreover, the S-wave velocity at the top surface to the depth of 5 m was so slow as 80 m/s. We continue to estimate the distribution of the soft sediments and lava structure beneath them, to elucidate how fissures were generated in this area.

The characteristics of damaged buildings due to the 2016 Kumamoto Earthquake in Mashiki town

*Takahito Kuroki[1], Nozomi Iso[2]

1. Faculty of Education, Univ. of Teacher Edu. Fukuoka, 2. Department of Human Sciences, Seinan Gakuin University

The 2016 Kumamoto Earthquake caused huge damages to many buildings and infrastructures in Kumamoto city, Mashiki town and others inside of the area in Kumamoto plain, central Kyushu. These damages occurred along two active fault zones, Futagawa fault zone and Hinagu fault zone. Many faults or co-seismic surface ruptures appeared to large damages on many buildings in central Mashiki town, because this area situated a cross zone on the extended part of the two fault zone. This study reports some characters of damaged buildings which were obtained by the observation of more than 3,600 buildings in 1.43 km^2 of central Mashiki and reports some characters of more than 330 co-seismic surface ruptures occurred there.

We checked 6 items of each building character in the study area. They are damage degree, type of building use, building age, roofing material, building material and tilted building direction. The damage degree of buildings was classified to 5 sections, counted large damaged 409, middle damaged 464, small damaged 575, covered roof 349 and no damaged 1,427. The type of building use was separated to 3 sections, counted residence 2,456 buildings, warehouse 770 buildings and nothing or removed 352 buildings. The building age was classified to 4 sections, counted very old 118 buildings, old 1,652 buildings, new 1,172 buildings and very new 281 buildings. The roofing material was separated to 3 sections, counted ceramic tile 1,472 buildings, slate one 706 buildings and other 1,045 buildings. The building material was divided to 2 sections, counted combustibleness 2,439 buildings and incombustibleness 813 buildings. The tilted building direction was measured, counted the north direction 232 buildings, the east direction 374 buildings, the south direction 442 buildings and the west direction 442 buildings.

We calculated the percentage of degree of damage for each item, and then we found the characters of damaged buildings as follows. From the building use type analysis, we found the damage ratio of residence was higher than that of warehouse. From the roofing material analysis, we found the damage ratio of ceramic tile was higher than that of slate one or other. From the building material analysis, we found the damage ratio of combustibleness is higher than that of incombustibleness. From the tilted building direction analysis, we found majority of the direction was the east-west which showed close direction to the strike of the earthquake faults. From the damage degree analysis, we found the damage ratio was high when the building was old and the ratio was low when the building was new. In other words, the degree of building damage levels was lower when the building was new.

From these analyses, we reclassified damage degree of building into 5 degrees from 1 to 5, arranged from easy to heavy. Distributional map of the damage degree was made by using a spatial-filtering GIS function. Therefore the severely damaged zone was indicated clearly in this area. It is important that earthquake surface faults and/or co-seismic surface ruptures concentrated at the marginal area of this zone.

Keywords: the 2016 Kumamoto Earthquake, damaged building, earthquake fault, GIS

Spatial distribution analysis of buildings with middle-level damage following Kumamoto earthquakes in 2016

*Hiroto Nagai[1], Ryo Natsuaki[1]

1. Japan Aerospace Exploration Agency

A series of M6-7 class earthquakes were initiated on April 14, 2016 around Kumamoto. Following these events, many buildings were covered with plastic sheets to facilitate repair, making their spatial distribution heterogeneous. By assumes this spatial heterogeneity of building damage, this study clarifies the spatial distribution of buildings. In addition, relationships with geomorphological factors are considered, and a preliminary method for early recognition of damage distribution using a remote sensing technique is determined.

Google Earth is a well-known digital earth software used globally. In this study, three-dimensional post-quake building models located around Kumamoto city taken by aerial photography a few weeks after the quakes were identified from Google Earth. The images enabled viewing from all angles; roofs with plastic sheets were visually identified, mostly as blue, green, and white, and their locations were recorded and defined as "middle-damaged building (MDB)". Such buildings were the ordinal residences of individual families and also commercial multiple-floor buildings. Multiple sheets on a single building were regarded as one MDB. Green houses on farms, exterior objects, vehicles, and buildings under construction were excluded from analysis. In addition, digitized information of the original and whole building distribution was obtained from the Geospatial Information Authority of Japan (GSI) (i.e. two-dimensional polygons of building outlines).

Geospatial statistics show 15675 MDBs out of a total of 165177 buildings (9.5%). Spatial distribution on a GSI geomorphologic map shows that all buildings are mainly distributed as follows: 40.2% on terrace, 14.8% on alluvial fan, 15.0% on flood plain, and 8.0% on natural levee; whereas the distribution of MDBs is as follows: 13.0% on terrace, 5.5% on alluvial fan, 5.3% on flood plain, and 6.7% on natural levee. These results suggest that buildings on a terrace have are relatively more likely to suffer damage compared to those on an alluvial fan, flood plain, or natural levee. Although catastrophic devastation is significantly identified near the moved active fault (e.g. Mashiki town in Kumamoto), the occurrence of moderate damage (where buildings could possibly be reused after repair) has a remarkable correlation with geomorphologic condition type. Further discussion is expected in relation to characteristics of the earthquake mechanism.

Significant surface change causes a decrease in coherence in the interferometric processing of synthetic aperture radar, and there is thus less similarity between the reflected phases. This method is used to determine the distribution of damaged buildings. Normalized coherence decrease (NCD) is calculated using PALSAR-2 data observed on November 30, 2015, March 7, 2016 (both for pre-quake), and on April 18, 2016 (post-quake). The frequency of NCD values on MDBs and those for whole buildings show statistically different distributions within histograms. This result shows that moderate damage occurring to the roofs of buildings causes a higher NCD. Further improvement is thus required to detect individual damaged buildings in a case of hazard response.

Keywords: Remote sensing, ALOS-2, Geomorphology, Coherence

The running photographic investigation by an automobile for estimating building damages of 2016 Kumamoto earthquakes

*Shohei Naito[1], Hiromitsu Nakamura[1], Hiroyuki Fujiwara[1]

1. National Research Institute for Earth Science and Disaster Resiliense

It is crucial to develop methods for get a prompt overview of the damage situation soon after the earthquake, in terms of supporting decision-makings quickly. For this reason, we have been developing the Japan real-time information systems for earthquake (J-RISQ).

Both in cases of the foreshock (M6.5) on April 14 and the main shock (M7.3) on April 16, J-RISQ have published final reports of 2016 Kumamoto earthquakes which includes estimated distributions per 250-meter meshes of seismic intensities, exposed populations, and building damages, approximately within 10 minutes. These estimations indicate a belt of destructive area adjacent to Mashiki town, and also correspond approximately to actual damaged area. However, it still have several problems like estimated results of building damages were overestimated, and it have not been considerable for sequential shakings of aftershocks.

To verify and improve the real-time damage estimation methods, we have to gather information of the actual damage caused by 2016 Kumamoto earthquakes by multiple ways such as field investigations, aerial photographs, running investigations by automobiles.

In this paper, we are going to describe about the running photographic investigation by an automobile. We have performed running surveys from April 17th to 28th, in Kumamoto city, Nishihara village, Mifune town, Kashima town, Mashiki town, and Kousa town. The total running distances are 576 km.

We have acquired digital images every 5 meters with 6 cameras installed inside the automobile, additionally, the location and time of these cameras are synchronized with GPS. Then, we have extracted the 7,584 photographs of buildings from 571,700 photos. In the next place, we have chosen 593 total collapsed buildings by the standard of classification chart of the building damage released by Cabinet Office.

As a result, the distribution of total collapsed buildings are within the rage of 1 km around surface ruptures caused by 2016 Kumamoto earthquakes. These distribution is also coordinate with the damage concentrate area estimated by field investigations and aerial photographs.

From now on, we are going to develop methods for estimating building damages by way of the machine learning with extracted damage photographs. These methods would be actualize more detail and immediate damage estimation.

References:

H.Nakamura,H.Fujiwara,T.Kunugi,S.Aoi,S.Senna,I.Takahashi,S.Naito,and H.Azuma: Development of real-time earthquake damage information system in Japan, 16th World Conference on Earthquake, Santiago Chile, 2017.

Y. Shirahama, M.Yoshimi, Y.Awata, T.Maruyama, T.Azuma, Y.Miyashita, H. Mori, K.Imanishi, N.Takeda, T.Ochi, M.Otsubo, D.Asahina, and A.Miyakawa, "Characteristics of the surface ruptures associated with the 2016 Kumamoto earthquake sequence, central Kyushu, Japan", Earth Planets and Space(2016), 68:191.

Keywords: Kumamoto earthquake, Building damage, Running investigation, Photographic interpretation,
          Active fault
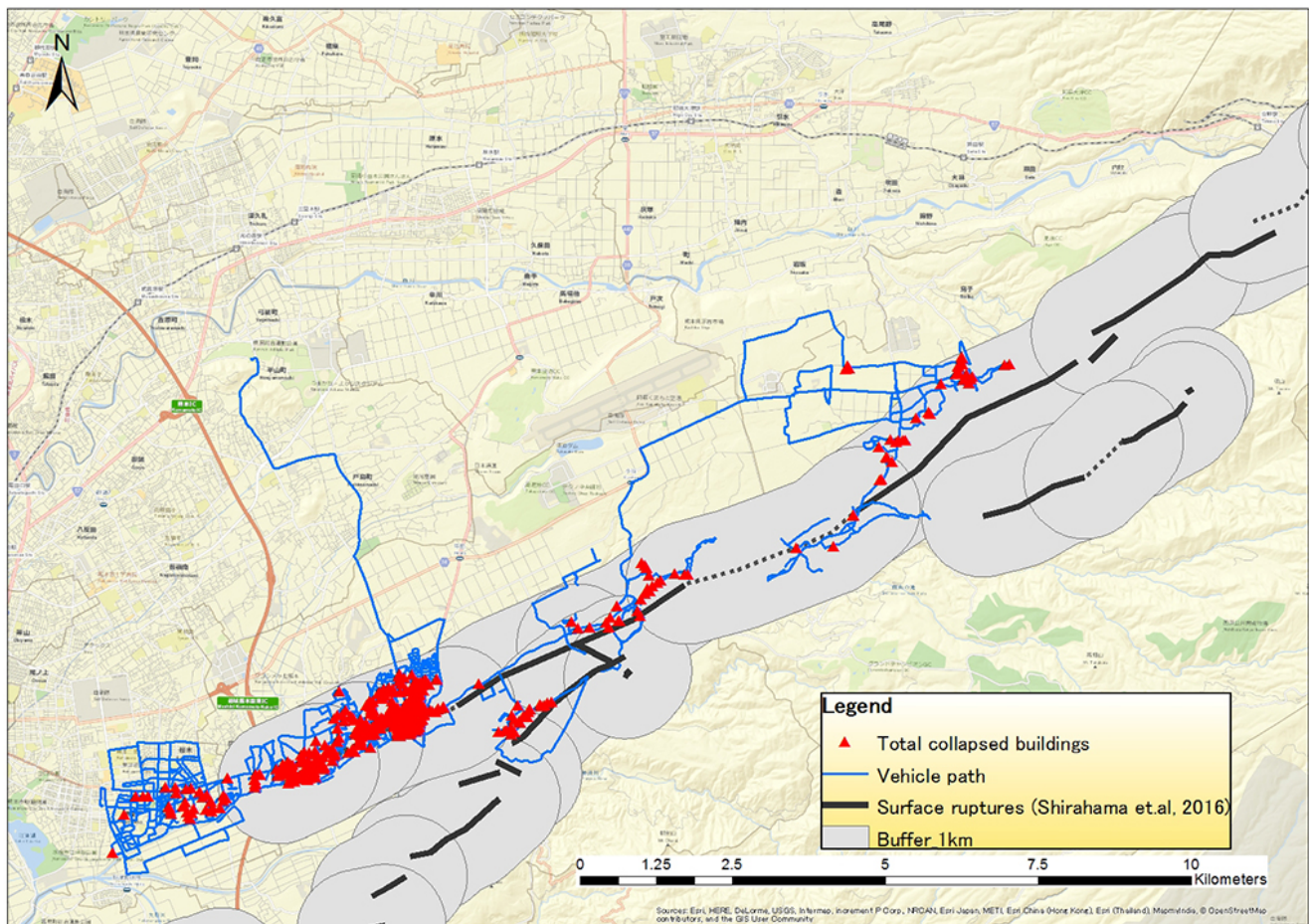
Feature of the building damage of Kumamoto earthquake by airphoto-interpretation

*naokazu momma[1], hiroyuki fujiwara[2], hiromistu nakamura[2], takuma saeki[2], hiroyuki shimomura[1], tetuya yamada[1], seiji fujisawa[1]

1. PASCO Co, 2. National Research institute for Earth science and Disaster resilience

In Kumamoto-ken, an earthquake of magnitude 6.5 (fore-shock) occurred on April 14, 2016 and an earthquake of magnitude 7.3 (main shock) occurred on April 16. Mashiki-machi and Nishihara-mura recorded seismic intensity 7 by this earthquake, and enormous building damageoccurred.WeinvestigatedbuildingdamagetargetedforMashiki-machi, Nishihara-mura, Kumamoto-shi, Uto-shi, Uki-shi, Aso-shi, Kashima-machi, Kosa-machi, Ozu-machi and the minami Aso mura. Investigation method is the way by which watch reads building damage from the air photo taken a picture of after fore-shock and main shock. The large (collapse and tear), tte medium (partial destruction) and the small (part damage) and without divided the degree of the damage into reading of building damage . When the distribution of the building of the damage large by the main shock is seen, the damage large is distributed over the northeast-southwest direction successively from the south Aso village to Kumamoto-shi Higashi-ku. Mashiki-machi excels with about 1,400 houses, and have a lot of number of houses of the damage large. Nishihara-mura, Kumamoto-shi Higashi-ku, Kashima-machi and the south Aso village are 150-180 houses.In Mashiki Town, the about 85%number of damage large is estimated by seismic intensity 7, the remaining is seismic intensity6strong. We calculated the collapse rate of the damage size of 250 m mesh.Looking at the relationship with constant seismic intensity, the collapse rate tends to increase as the estimated seismic intensity increases.However, even with the same seismic intensity value, the collapse rate has the largest width to the minimum and maximum.

Keywords: Kumamoto earthquake, airphoto-interpretation, building damage, seismic intensity, collapse rate

Relationship between building damage and liquefaction sites during the 2016 Kumamoto Earthquake

*Ozawa Kyoko[1], Shigeki Senna[1], Hiroyuki Fujiwara[1]

1. National Research Institute for Earth Science and Disaster Prevention

During the 2016 Kumamoto Earthquake that occurred on April 14 and 16, 2016, liquefaction occurred over the large area. We checked a relation between a liquefaction sites and building damage levels in this study.

We judged liquefaction sites at the mesh size of 50m using high-resolution aerial photographs, and found liquefaction for about 5,800 meshes. Comparing this result with building damage data, we checked a relation between them.

It seems that building damage is heavier at liquefaction sites in Kumamoto city. This indicates that liquefaction can affect building damage levels also in other areas.

Liquefaction was caused over the large area due to the Kumamoto earthquake. We checked a relation between liquefaction sites and building damage levels based on each investigated results. Then, it was found that building damage tended to be heavier due to liquefaction in a certain area. It is necessary to investigate the relation in more details using other types of liquefaction data from now on.

Keywords: the 2016 Kumamoto Earthquake, liquefaction, building damage

Simulation of building damage distribution by the 2016 Kumamoto Earthquake by use of limited information on real damage

*Akihiro Kusaka[1,2], Hiromitsu Nakamura[1], Hiroyuki Fujiwara[1], Katsuhisa Kanda[2], Naokazu Momma[1]

1. National Research Institute for Earthquake Science and Disaster Resilience, 2. Kobori Research Complex Inc.

1. Introduction

In case of widely spread disaster such as a great earthquake, a disaster information system is under development to gather and estimate the whole damage situation in "real-time" in order to support decision-making for initial corresponding. In a very short time after an earthquake occurs, the system estimates ground motion distribution by each 250m regional mesh by interpolating strong motion records which are gathered by nationwide observation station networks, K-NET and KiK-net etc. Then, it combines the estimated ground motion distribution with prepared fragility functions and exposure data to estimate the number of damaged houses. Moreover, a method to improve the estimated accuracy is being developed, by use of actual damage information on limited areas as "observation" in Bayesian updating protocol. This report deals with numerical examples of the method.

2. Updating framework for estimation error in numbers of damaged houses

The system, at first, generates "immediate estimates" which is based on ground motion distribution and prepared fragilities and exposure data. In the estimation, errors of the parameters of fragilities are modeled as random variables. Then, the parameters of probability distributions are updated by Bayesian protocol by use of actual damage information such as the real numbers of damaged houses in some particular areas.

3. Actual damage information read from aerial photographs

This study uses the numbers of damaged houses in each 250 m mesh as actual damage information. They are read by eyes from the oblique photographs took from a helicopter after occurrence of the Earthquake (Mw 7.3) on April 16th.

In the numerical examples, we use only a part of information; that on some selected meshes, in order to examine how to improve the estimation accuracy even with as small data as possible. The selecting process is as followings: 1. Chose meshes those include twenty or more houses from some districts, where are determined with reference to the estimated ground motion distribution. 2. Divide the chosen meshes into several groups based on geomorphography classification, which is determined for each 250m mesh. 3. Select at random almost same numbers of meshes from each of mesh groups.

4. Results

"Immediate estimate" by inputting ground motion distribution for the Mw 7.3 earthquake into the fragility functions used in damage estimates by Japan Cabinet Office (2012) overestimated the number of damaged houses by around four times of that reported for the whole suffered area. Several cases are examined for different information. The case the presented method works well is that using both information of Mashiki town, which represents most severely damaged areas, and that of Higashi-Ku, Kumamoto City, which represents typically suffered areas. The numbers of damaged houses read from ten meshes of each area can update the estimate to close to the reported numbers. On the other hand, in a case using information of twenty meshes only from Mashiki town the damage is still overestimated, and in a case with twenty meshes only from Higashi-Ku, Kumamoto City, the number is rather underestimated.

Acknowledgements

Keywords: Kumamoto Earthquake, Bayesian updating, post-earthquake assessment

Tomographic and gravimetric signatures of the fault system associated with the 2016 Kumamoto earthquake (M7.3), Japan

*ZHI WANG[1], Yoshio Fukao[2], Ayumu Miyakawa[3], Akira Hasegawa[4], Yasuko Takei[5]

1. Key Laboratory of Marginal Sea Geology at South China Sea Institute of Oceanology of CAS of China, 2. CEAT, Japan Agency for Marine-Earth Science and Technology, Yokohama, Japan, 3. Geological Survey of Japan, AIST, Tsukuba, Ibaraki, Japan, 4. Department of Geophysics, Tohoku University, Sendai , Japan, 5. Earthquake Research Institute, University of Tokyo, Tokyo, Japan

A series of shallow large earthquakes with the M_J7.3 mainshock (April 15, 2016) struck the Kumamoto area of Kyushu, Japan. The mainshock was a slip along the Futagawa Fault, a segment of the EW-running Oita-Kumamoto Tectonic Line. By this tectonic line the Beppu-Shimabara Graben is bounded sharply on the south, where NS-extensional crustal deformation is now taking place and earthquakes (including the 2016 aftershocks) are largely NS-dipping normal faulting. We conducted a seismic tomographic study for the crustal Vp and Vs anomalies using arrival time data from the Hi-Net stations in Kyushu. The most outstanding tomographic feature in this region is a belt of low Vp and Vs anomalies at depths of the upper crust geographically coinciding with the Beppu-Shimabara Graben (Fig.1). This belt is characterized by such an approximate equality that dVs/Vs ≈dVp/Vp (<0) in marked contrast to the relation in other regions or at greater depths where dVs/Vs < dVp/Vp (<0). This observation can be interpreted in terms of water-saturated, oblate-spheroid pores created by the extensional deformation of the upper crust in the Beppu-Shimabara Graben. The approximate equality between dVs/Vs and dVp/Vp holds if the aspect ratio α of pore geometry is either ˜0.04 (flat pore) or ˜1 (spherical pore). Once α is specified, the water volume fraction and hence density anomaly dρ / ρ (<0) can be calculated from the observed dVp/Vp or dVs/Vs. We calculate Bouguer anomalies from the density anomaly distribution so obtained. The Bouguer map calculated for spherical pores shows a remarkable negative anomaly belt in agreement with the Beppu-Shimabara Graben signature on the observed Bouguer map (Fig.2). The agreement is very poor if pores are flat. This result demonstrates a unique role of gravity data when it is combined with seismic P and S wave data. The Oita-Kumamoto Tectonic Line, including the Futagawa Fault, is a bimaterial boundary, to the north of which the material is slower in both Vp and Vs and less dense. The rupture process of the 2016 Kumamoto earthquake was likely to be affected by this bimaterial nature of the fault.

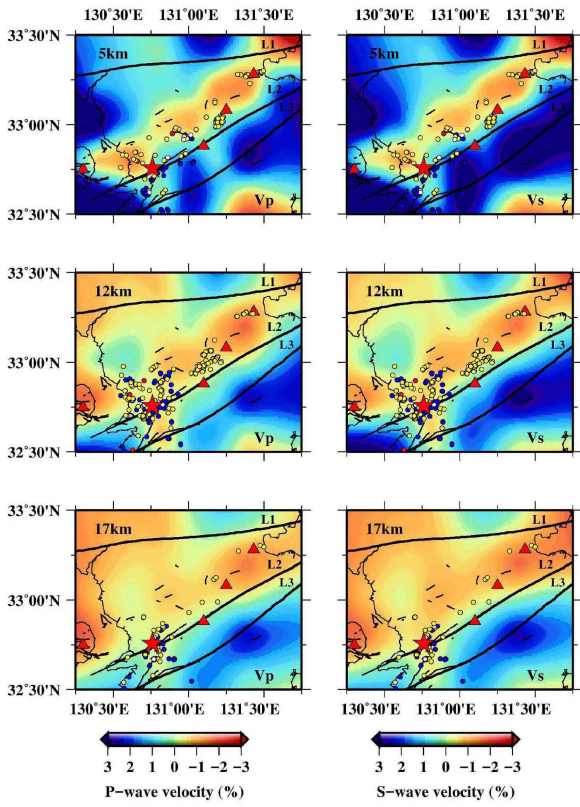Keywords: 2016 Kumamoto earthquake, Fluid intrusion, Multiple parameter imaging

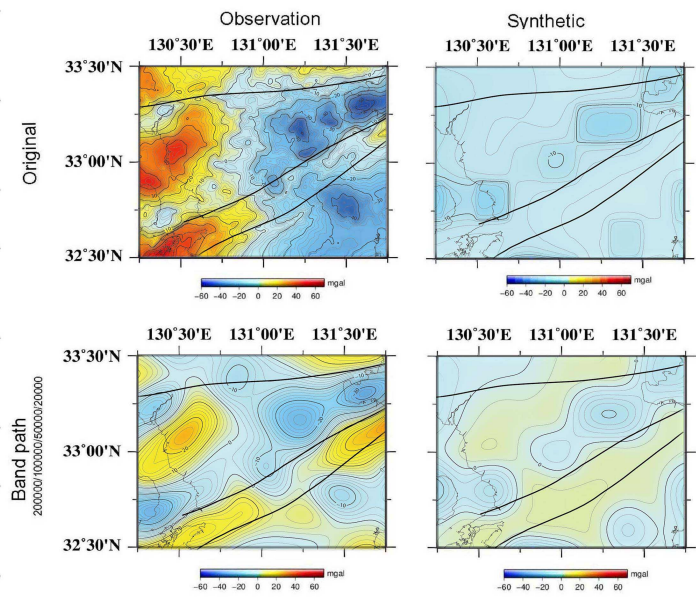Figure 1: Vp and Vs anomalies at three depths of the upper crust

Figure 2: Observed and synthetic Bouguer anomaly maps. Synthetic maps are shown for a case of water-saturated spherical pores. Top: unfiltered maps. Bottom: bandpass-filtered maps.

Earthquake-volcano interactions in the 2016 Kumamoto earthquake area

*Dapeng Zhao[1], Zewei Wang[1], Xin Liu[1], Yukihisa Nishizono[2], Hirohito Inakura[2]

1. Department of Geophysics, Tohoku University, 2. West Japan Engineering Consultants, Inc.

The 16 April 2016 Kumamoto earthquake (M 7.3) took place in north-central Kyushu where several active arc volcanoes exist (e.g., Aso, Kuju, Tsurumidake, and Unzen) due to the active subduction of the Philippine Sea (PHS) plate beneath the Eurasian plate. On 8 October 2016 the Aso volcano erupted, which may be related to the occurrence of the Kumamoto earthquake. Many previous studies have suggested that earthquakes and volcanoes can interact with each other in subduction-zone regions. To investigate the possible earthquake-volcano interaction in Kyushu, in this work we study the three-dimensional seismic velocity (Vp, Vs) and attenuation (Qp and Qs) structures in the source area of the 2016 Kumamoto earthquake (M 7.3) using ~62,000 P and S wave arrival times and 48,000 t* data measured from digital seismograms of 742 local shallow and intermediate-depth earthquakes recorded by the Hi-net stations in Kyushu Island. Our results show that significant low-velocity (low-V) and low-Q (high attenuation) anomalies exist in the crust and mantle wedge beneath the volcanic front and back-arc area, which reflect hot and wet anomalies caused by convective circulation in the mantle wedge and fluids from the PHS slab dehydration. The PHS slab is imaged clearly as a high-velocity (high-V) and high-Q (low attenuation) dipping zone in the upper mantle. The 2016 Kumamoto earthquake occurred in a high-V and high-Q zone in the upper crust, which is surrounded and underlain by low-V and low-Q anomalies in the lower crust and upper mantle. These results suggest that the 2016 Kumamoto earthquake took place in a brittle seismogenic layer in the upper crust, but its rupture nucleation was affected by fluids and arc magma ascending from the mantle wedge. In addition, a prominent low-V and low-Q zone is revealed in the forearc mantle wedge beneath Kyushu, which reflects serpentinization of the forearc mantle due to abundant fluids from the PHS slab dehydration. These results suggest that arc magma and fluids play an important role in the generation and nucleation processes of large crustal earthquakes which can in turn rupture the active faults and produce new cracks in the crust, facilitating the volcanic eruption. As a result, earthquake-volcano interactions take place in north-central Kyushu.

Keywords: Kumamoto earthquake, volcanoes, Kyushu, subduction zone, Philippine Sea plate

Yufuin fault cause an earthquake with an intensity of lower 6 in Beppu

*tatsurou yoshimura[1]

1. Meidai Co., Ltd.

Another earthquake of M5.7 occurred in the Oita Prefecture central part 32 seconds after the main shock on April 16, 2016. The intensity 6 lower was observed in Beppu City and the Yufuin city of the northeast about 80km from Kumamoto. Ufuin fault is distributed in aftershock area in the Oita Prefecture central part. The setting of the active fault length was examined by the comparison between scenario magnitude from γ-ray survey results and actuaiiy occurred magnitude.

Keywords: Earthquake in the Oita Prefecture central part, Yufuin fault, Fault length